Activation energies and localization in the fractional quantum Hall effect

G. S. Boebinger*
Department of Physics and Francis Bitter National Magnet Laboratory, Massachusetts Institute of Technology, Cambridge, Massachusetts 02139

H. L. Stormer†
AT&T Bell Laboratories, Murray Hill, New Jersey 07974-2070

D. C. Tsui†
Department of Electrical Engineering and Computer Science, Princeton University, Princeton, New Jersey 08544

A. M. Chang†
AT&T Bell Laboratories, Holmdel, New Jersey 07733-7020

J. C. M. Hwang,‡ A. Y. Cho, and C. W. Tu
AT&T Bell Laboratories, Murray Hill, New Jersey 07974-2070

G. Weimann
Forschungsinstitut der Deutschen Bundespost beim Fernmeldetechnische Zentralamt, D-6100 Darmstadt, Federal Republic of Germany
(Received 29 April 1987)

This paper summarizes an extensive study of the temperature dependence of magnetotransport in the fractional quantum Hall effect in GaAs-$Al_xGa_{1-x}As$ heterostructure devices of varying mobility and density. For devices with electron mobility $400\,000 \lesssim \mu \lesssim 1\,000\,000$ cm^2/V s, we find a single activation energy, $^3\Delta/2$, in the longitudinal transport coefficients, σ_{xx} and ρ_{xx}, for Landau-level filling factors $\nu=\frac{1}{3}$, $\frac{2}{3}$, $\frac{4}{3}$, and $\frac{5}{3}$, with a magnetic field dependence which is vanishingly small for $B \lesssim 5.5$ T and increases to $^3\Delta \sim 6.8$ K at $B=30$ T. The observed $^3\Delta$ is smaller by more than a factor of 3 than either the unbound quasiparticle-quasihole pair-creation energy gap or the magneto-roton energy gap, calculated for an ideal two-dimensional electron system. Observations for devices of mobility $\mu_0 \approx 300\,000$ cm^2/V s yield even smaller $^3\Delta$. Adequate fitting of all our results requires inclusion of finite electron layer thickness and disorder, with the effect of decreasing the energy gaps and providing a finite magnetic field threshold. At low temperatures and high magnetic fields, deviations from activated conduction are observed. These deviations are attributed to two-dimensional hopping conduction in a magnetic field. Samples of sufficiently low mobility, $\mu_0 \lesssim 150\,000$ cm^2/V s exhibit no evidence of activated conduction. Rather, the transport is qualitatively consistent with two-dimensional hopping alone. Studies at Landau-level filling factors $\nu=\frac{2}{5}$ and $\frac{3}{5}$ also yield a single activation energy, $^5\Delta/2$, with a weak magnetic field dependence. Experimentally, we find $^5\Delta/^3\Delta \sim 0.4$, compared with an expected ratio of 0.28 from simple theoretical considerations.

I. INTRODUCTION

In recent years, much of the experimental work on the fractional quantum Hall effect[1] (FQHE) has sought to determine the magnitude of the energy gaps above the electron ground states, existing at fractional filling of the lowest Landau level. The experiments involve determining activation energies from magnetotransport experiments[2–11], although very recently a spectroscopic determination has been reported.[12] In this paper we summarize our extensive study of the magnetotransport energy gap in the FQHE regime, including an expansion upon our initial activation energy results,[6,7] recent experiments on the dependence of the activation energies on sample channel width and mobility, and results on the transport behavior of low-mobility samples which appear qualitatively consistent with hopping conduction.

The FQHE and integral quantum Hall effect (IQHE) are observed in magnetotransport on two-dimensional (2D) systems, sharing the hallmark features of plateaus in the Hall resistivity ρ_{xy} at certain Landau-level filling factors $\nu=nh/eB$ (n is 2D electron density, eB/h is Landau-level degeneracy), coexistent with zero resistance states in the diagonal resistivity ρ_{xx}. However, the underlying physics of the two effects are markedly different. Whereas the IQHE results from independent particles quantized by a magnetic field, the FQHE is a many-body effect, currently understood as arising from the existence of finite-energy gaps above a series of novel quantum fluid ground states at fractional Landau-level filling factors $\nu=p/q$ (p and q are integers and q is odd).[13–16] In the context of this study, we focus on the

excitations above these ground states.

For the ideal 2D electron system in which electron layer thickness, higher Landau-level mixing, and disorder are neglected, various calculations have yielded a fairly consistent picture of the FQHE excitations at $\nu=\frac{1}{3}$. These calculations demonstrate that the dispersion relation of the elementary excitations has a minimum at a finite wave vector. Girvin *et al.*[17] obtained this result by employing a single-mode approximation, analogous to Feynman's theory for superfluid helium; Haldane and Rezayi[18] and, recently, Fano *et al.*[19] report numerical studies on finite electron systems. The minimum-energy "magneto-roton" (MR) excitation corresponds to an electrically neutral excitation with momentum $k\sim 1.4 l_0^{-1}$ and excitation energy $\Delta_{\rm MR}\sim 0.08 e^2/\epsilon l_0$ [e is electron charge, $\epsilon=12.8$ (for GaAs) is the dielectric constant, and $l_0=(\hbar/eB)^{1/2}$ is the magnetic length]. For $k\rightarrow\infty$, the dispersion relation approaches the more energetic pair-creation energy $\Delta_{\rm QP}$ of spatially separated fractionally charged quasiparticles and quasiholes. At finite temperatures T (but $kT<\Delta_{\rm MR},\Delta_{\rm QP}$), the electronic system consists, to a very good approximation, of the ground state with a small number of thermally activated excitations (magnetorotons, as well as quasiparticles and quasiholes) modifying the transport properties of the system. In particular, the diagonal conductivity σ_{xx} [and, consequently ρ_{xx}; due to $\rho_{xx}=\sigma_{xx}/(\sigma_{xx}^2+\sigma_{xy}^2)\approx\sigma_{xx}/\sigma_{xy}^2\propto\sigma_{xx}$] is expected to be proportional to the number of thermally activated, electrically charged quasiparticles and quasiholes. Hence, the experimentally determined activation energy of σ_{xx} and/or ρ_{xx} provides a measure for the value of the gap in the elementary excitations above the FQHE ground state, in complete analogy to the IQHE, where the same quantity reflects the Landau-level splitting $\hbar\omega_c$. Because the magneto-roton is electrically neutral, it may not be the excitation of interest experimentally. It is likely that our dc transport experiments identify the more energetic pair creation of spatially separated fractionally charged quasiparticles and quasiholes. Theoretical calculations[17–21] yield a quasiparticle pair-creation energy $\Delta_{\rm QP}\sim 0.10 e^2/\epsilon l_0$. Although we interpret the experimental activation energies for $\nu=\frac{1}{3}$, $\frac{2}{3}$, $\frac{4}{3}$, and $\frac{5}{3}$ in terms of quasiparticle pair creation, we will discuss both $\Delta_{\rm QP}$ and $\Delta_{\rm MR}$ in conjunction with experimental results. For $\nu=\frac{2}{5}$ and $\frac{3}{5}$, a similar level of consistency in the calculations of the excitation energies still does not exist. However, it is expected[16] that the energy gaps will scale roughly with the charge of the quasiparticle, $e^*=e/q$ at $\nu=p/q$. Thus, approximately,

$$\Delta\propto(e^*)^2/\epsilon(l_0^*)\propto q^{-5/2}B^{1/2}\ .$$

For $\nu=\frac{2}{5}$ and $\frac{3}{5}$, this corresponds to $\Delta_{\rm MR}\sim 0.02 e^2/\epsilon l_0$ and $\Delta_{\rm QP}\sim 0.03 e^2/\epsilon l_0$.

II. DEVICE CHARACTERISTICS

The samples are modulation-doped GaAs/AlGaAs heterojunctions grown by molecular-beam epitaxy on semi-insulating Cr-doped substrates. The 2D electron layer forms in the GaAs at the interface with the undoped $Al_xGa_{1-x}As$ spacer layer. The inclusion of this undoped spacer layer significantly enhances the electron mobility by spatially removing the 2D electrons from the ionized Si donors.[22,23] Electrical contacts to the 2D electron layers are made by diffusing indium through the $Al_xGa_{1-x}As$ layers at 450 °C for 5–10 min in a hydrogen atmosphere. Table I contains the sample parameters for the specimens studied. Both the density and mobility of the 2D layer can be altered via application of a voltage bias to a backside electrode.[24] To avoid eddy-current heating, the electrodes consist of 500 Å of titanium and 1000 Å of gold evaporated on a GaAs wafer. As expected from a simple capacitor model, the electron density varies roughly linearly with bias for biases up to ±700 V, after which saturation is observed. Biases of 700 V result in density increases by as much as 80%. This gate bias simultaneously alters the electron mobility, following $\mu\propto n^{\chi}$, where $1.5\lesssim\chi\lesssim 1.7$ for our specimens (Fig. 1).

Many of the samples for resistivity measurements are

TABLE I. Sample parameters: x is the Al concentration; $d_{\rm Si}$ is the Si-doped $Al_xGa_{1-x}As$ layer thickness; $N_{\rm Si}$ is the Si-doping concentration; $d_{\rm spacer}$ is the $Al_xGa_{1-x}As$ spacer-layer thickness; n_0 and μ_0 are the 2D electron density and mobility, both given for zero gate bias.

Sample	x	$d_{\rm Si}$ (Å)	$N_{\rm Si}$ (10^{18} cm^{-3})	$d_{\rm spacer}$ (Å)	n_0 (10^{11} cm^{-2})	μ_0 (10^3 cm^2/V s)
A	0.30	400	2.0	370	1.5	600
B	0.30	400	2.0	370	1.5	600
C	0.30	400	2.0	370	1.6	600
D	0.30	400	2.0	275	2.5	300
E	0.30	400	2.0	370	1.5	600
F	0.37	360	0.8	300	2.7	1100
G	0.39	290	0.9	370	1.5	500
H	0.30	800	1.0	425	1.9	79
I	0.30	800	1.0	425	2.0	72
J	0.30	380	0.9	170	2.5	140
K	0.30	400	2.0	370	1.5	600
L	0.30	400	2.0	370	1.5	600
M	0.30	400	2.0	275	2.5	300

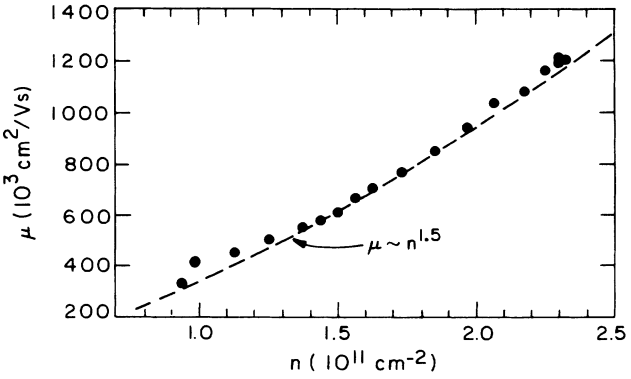

FIG. 1. Density dependence of the mobility for a typical sample.

etched in Hall bridge patterns [Fig. 2(a)] with channel dimensions of ~ 0.5 mm $\times$ ~ 3.0 mm, typically. The exception is sample *G*, which has Hall bridge channel dimensions of 11 μm $\times$ 450 μm. Several resistivity samples were not etched and simply consist of indium contacts positioned as a crude Hall bridge around the edges of the sample [Fig. 2(b)], normally ~ 1.5 mm $\times$ ~ 3.0 mm in size. No difference in the data is observed between the etched and the crude Hall bridge samples. The conductivity samples resemble the unetched resistivity samples with the addition of interior indium contacts [Fig. 2(c)] to provide a "quasi-Corbino" geometry, where σ_{xx} is measured between an interior contact and any other contact.

III. EXPERIMENTAL TECHNIQUES

The magnetotransport experiments utilize a dilution refrigerator designed specifically for the hybrid magnet at the Francis Bitter National Magnet Laboratory. The mixing chamber of the refrigerator is greatly elongated to meet the conflicting requirements of (1) a large cross-sectional area at the ^{3}He-^{4}He phase boundary for effective cooling and (2) the restricted bore size of the hybrid magnet. The ^{3}He-^{4}He phase boundary is located at the top of the mixing chamber, outside the bore of the magnet. Below this, the mixing chamber has a long tail (1 cm diam $\times$ 70 cm), with a ^{3}He return line which extends to the bottom. In this manner, the cold ^{3}He circulation is directed past the samples immersed in the dilute phase nearly 70 cm below the phase boundary. This radical design dramatically reduces the ability of the refrigerator to handle a heat load near the samples from 75 μW to 10 μW at 100 mK. All parts of the mixing chamber except the top portion are fabricated from epoxy to avoid ruinous eddy-current heating from the ac components of the magnetic field. Only with such care are we able to achieve a temperature of 65 mK at 30-T magnetic field.[25]

Accurate thermometry in a dilution refrigerator in high magnetic fields is difficult. Our sample temperature is determined by the resistance of a calibrated 220 Ω (at 300 K) Speer resistor located near the samples. The magnetoresistance of this thermometer is consistent with the results of Naughton *et al.*[26] The uncertainty in the magnetoresistance correction accounts for roughly half of the reported uncertainties in the activation energies.

The experiments involved standard lock-in detection techniques, typically utilizing frequencies between 2 and 23 Hz. When measuring the small signals at the lowest temperatures, the lower frequencies experience fewer problems with phase shifts, due apparently to capacitive components of the indium contacts which become increasingly pronounced at large *B* field. Typical sample excitations are 100 nA for resistivity measurements and 10 mV for conductivity measurements. At these excitations no electron heating effects are observed even at the lowest temperatures.

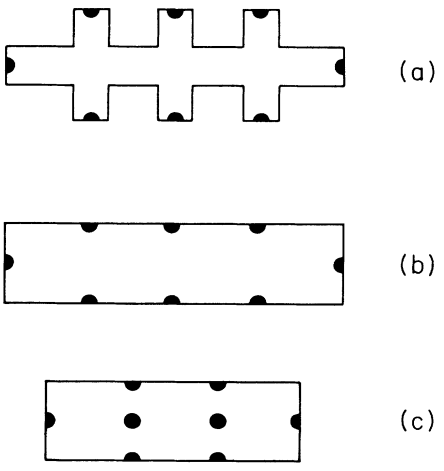

FIG. 2. Sample geometries. (a) Photolithographically defined Hall bridge; (b) crude Hall bridge defined by cleaving samples to appropriate size; (c) "quasi-Corbino" geometry for direct measurement of σ_{xx}.

IV. DATA PRESENTATION AND ANALYSIS

A. High-mobility results

The data sets consist of the magnitude of ρ_{xx} or σ_{xx} measured at the minimum corresponding to a given fractional filling factor. These are measured over a range of temperature within the practical limits of our dilution refrigerator: 100 mK $\lesssim T \lesssim$ 1.5 K. Figure 3 shows six sets of data for $\nu = \frac{1}{3}, \frac{2}{3}$, and $\frac{5}{3}$ which illustrate the evolution of the data with magnetic fields ranging from 5.9 to 29.0 T. At low magnetic fields the data follow a straight line, indicating activated conduction. The activation energy $\Delta/2$ expressed in kelvins is determined from

$$\rho_{xx}(T) = \rho_0 \exp(-\Delta/2T)$$

and

$$\sigma_{xx}(T) = \sigma_0 \exp(-\Delta/2T) .$$

As defined here, Δ represents a quasielectron-

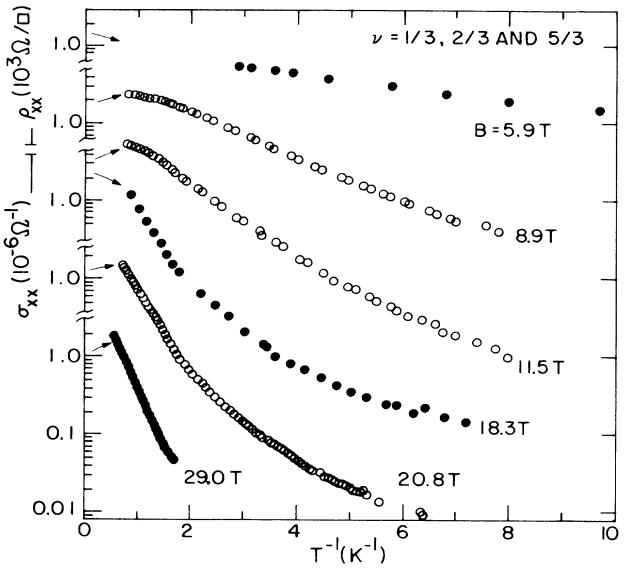

FIG. 3. Overview of temperature dependence of the minima in σ_{xx} and ρ_{xx} for magnetic fields from 5.9 and 29.0 T. The data represented by open and solid circles are from $\nu=\frac{2}{3}$ and $\frac{1}{3}$, respectively, with the exception of the data at 5.9 T from $\nu=\frac{5}{3}$.

quasihole pair-creation energy, in analogy with thermal activation of electron-hole pairs in semiconductors. (Note that this definition differs by a factor of 2 from Δ's defined in many of the referenced papers.)

Data taken at magnetic fields between 6 and ~ 10 T indicate only activated conduction over the experimental temperature range. An example is shown in Fig. 4 for $B=8.9$ T. The deviation in ρ_{xx} from a simple activated behavior at high T results from the fact that the weakly developed minimum resides on top of a slightly temperature-dependent background. At $B\sim 10$ T, a deviation from activated behavior at the lowest temperatures becomes observable and increases as the magnetic field is increased. Figure 4 shows the substantial deviation for $B=20.8$ T. Data at high magnetic fields exhibiting the low-T deviation fit very well over the entire temperature range to a sum of formulas representing an activated conduction which dominates at high T and hopping conduction which dominates at low T (solid line in Fig. 4 for $B=20.8$ T). This model is motivated by the phenomenological understanding that the quasiparticles in the FQHE away from the band center become localized in the presence of disorder, in analogy to the localization of electrons in the IQHE.[27,28] It is very important to note that the data are not consistent with the assumption of hopping conduction as the exclusive conduction mechanism over the entire experimental temperature range.

The formula used to model the hopping conduction in a magnetic field is derived by Ono[29] for electrons,

$$\sigma(T)=\sigma_{\mathrm{Ono}}(T)\exp[-(T_{\mathrm{Ono}}/T)^{1/2}] ,$$

where

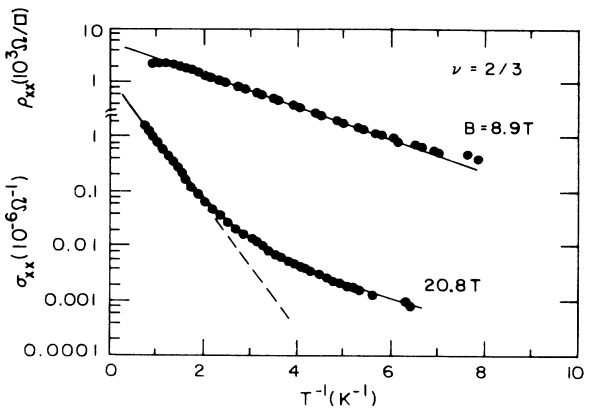

FIG. 4. Temperature dependence of the minimum at $\nu=\frac{2}{3}$. (a) At $B=8.9$ T, showing simple activated conduction. The solid line corresponds to a pair-creation energy of 1.3 K; (b) At $B=20.8$ T, showing the low-T deviation from activated conduction (dashed line corresponds to a pair-creation energy of 5.3 K). The solid line is the fit to a sum of activated conduction and Ono hopping conduction model.

$$\sigma_{\mathrm{Ono}}(T)=e^2\gamma_0/k_BT$$

and

$$k_BT_{\mathrm{Ono}}=\zeta_0/[l_0^2D(E_F)]$$

in which $D(E_F)$ is the density of states at the Fermi energy, γ_0 is a constant depending upon the electron-phonon coupling strength, the phonon density of states, and other material constants, and ζ_0 is a constant of order unity which is related to the critical concentration of the percolation problem. This formula results from considering the Mott hopping problem in 2D with Gaussian decay of the localized electron wave functions in the presence of a strong magnetic field: $\psi(r)\sim\exp(-r^2/2l_0^2)$. We assume that such a formula also applies to quasiparticle conduction, since the wave function is expected to be similarly localized.

Experimentally, the data is equally well fitted by two other candidate formulas to describe the low-temperature deviations. The first is the 2D Mott hopping formula,[30]

$$\sigma(T)=\sigma_{\mathrm{Mott}}(T)\exp[-(T_{\mathrm{Mott}}/T)^{1/3}] ,$$

where

$$\sigma_{\mathrm{Mott}}(T)=e^2\gamma_0D(E_F)^{1/3}/4(\pi\alpha k_BT)^{2/3}$$

and

$$k_BT_{\mathrm{Mott}}=(27\delta^2)/\pi D(E_F) ,$$

in which γ_0 is a constant depending on the electron-phonon coupling strength and δ is determined by the exponential decay of the localized electron wave function: $\psi(r)\sim\exp(-\delta r)$. The second is a low-temperature activated conduction,

$$\sigma_{xx}(T)=\sigma_2\exp(-\Delta_2/T) ,$$

where Δ_2 is a second, smaller activation energy. Possible candidates for a second activation energy have been discussed by Yoshioka[31] and Ihm and Phillips.[32]

Although the data on the high-mobility samples cannot distinguish among the three formulas, data on low-mobility samples, discussed below, are consistent only with the functional form of the Ono hopping formula. Also, the Ono formula has been found to well describe the experimental results from electrons at low temperatures in the IQHE.[27,28] For these reasons, we interpet the low-T deviations from activated conduction as due to hopping conduction of localized quasiparticles.

The fitted value of the high-T activation energy is only slightly dependent (5% typically) on the low-T formula chosen. Furthermore, this activation energy (dashed line in Fig. 4 at $B=20.8$ T) is consistent with the value determined from a straight line drawn through the high-T data, a simple analysis which ignores altogether any effects of a low-T conduction mechanism.

Our temperature data, a portion of which is contained in Fig. 3, indicates that the activation energy increases monotonically with increasing magnetic field. At a given low T the deviations from activated conduction increase with magnetic field. This behavior is likely due to the larger activation energies at higher magnetic fields. Therefore, as the magnetic field is increased, at a correspondingly higher temperature, the activated conduction component of ρ_{xx} and σ_{xx} decreases to become comparable in magnitude to a hopping conduction component. Experimentally, this crossover to hopping conduction occurs about 1.5 orders of magnitude below the conduction observed at 1.5 K. However, this field dependence of the onset of activated conduction may also result from the quasiparticle wave functions having smaller diameters at higher magnitude fields and, thus, localizing more easily.

In the ideal two-dimensional case, ρ_{xx} and σ_{xx} are simply related by matrix inversion,

$$\sigma_{xx}=\rho_{xx}/(\rho_{xx}^2+\rho_{xy}^2)\sim\rho_{xx}/\rho_{xy}^2\propto\rho_{xx}\ ,$$

where the proportionality holds in the ρ_{xx} minima ($\rho_{xx}\ll\rho_{xy}$). To verify that measurements of ρ_{xx} and σ_{xx} yield the same activation energy under experimental conditions, sample K was prepared with contacts for both ρ_{xx} and σ_{xx} measurements [Fig. 2(c)]. Figure 5 contains ρ_{xx} and σ_{xx} data measured simultaneously, at different frequencies (7 and 13 Hz, respectively) to avoid interference of the two signals and at particularly low excitations (10 nA and 1 mV, respectively) to avoid spurious effects due to electron heating. As the dashed lines in Fig. 5 indicate, the activation energies determined from the two curves are nearly identical. This result is at variance with remarks by Wakabayashi *et al.*[11] The slight difference between the two observed low-T deviations may be due to the fact that current paths are different for the ρ_{xx} and σ_{xx} measurements.

Figure 6 presents the experimental pair-creation energies $^3\Delta$ from the entire body of data from high-mobility samples on filling factors $\nu=\frac{1}{3}$, $\frac{2}{3}$, $\frac{4}{3}$, and $\frac{5}{3}$. This figure includes all the data from Boebinger *et al.*[6] except a data point at $B=28.0$ T and $^3\Delta=4.7$ K, found to correspond to much lower mobility. The data in Fig. 6 from sample A are from an early study of the $\frac{2}{3}$ minimum by Chang *et al.*[2] The error bars in the figure are the sum of two roughly equal components: the estimated errors from fitting the experimental data and the uncertainty in the magnetoresistance correction of the thermometry.

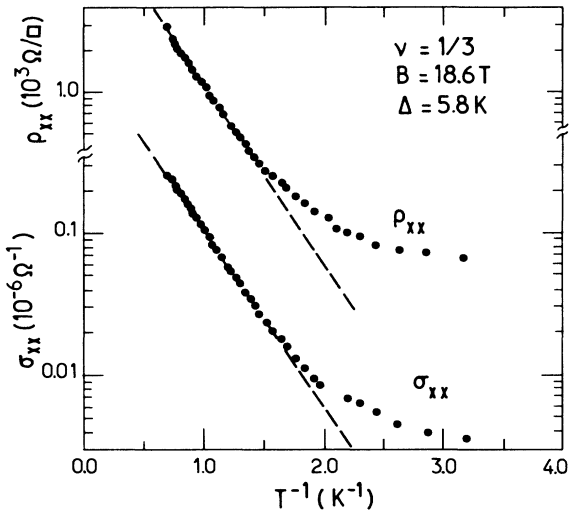

FIG. 5. Direct comparison of temperature dependences of ρ_{xx} and σ_{xx} at the $\nu=\frac{1}{3}$ minimum for $B=18.6$ T. The two sets of data were taken simultaneously on a single sample. The dashed lines correspond to a pair-creation energy of 5.8 K.

Four features of Fig. 6 should be stressed.

(1) There is no significant sample dependence for these samples with similar mobilities and growth parameters.

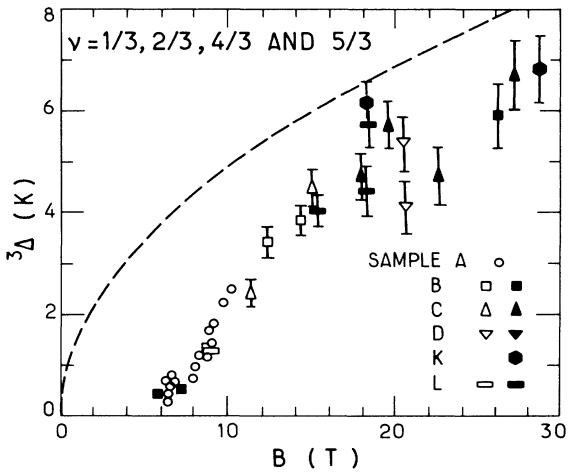

FIG. 6. The pair-creation energy for the third vs magnetic field for high-mobility samples. The open and solid symbols correspond to $\nu=\frac{2}{3}$ and $\frac{1}{3}$, respectively, except for the two solid squares at 5.9 and 7.4 T, which are from $\nu=\frac{5}{3}$ and $\frac{4}{3}$, respectively. The dashed line corresponds to $^3\Delta=0.03e^2/\epsilon l_0$, over a factor of 3 smaller than the calculated pair-creation energy gap for an ideal two-dimensional system.

In fact, the variation in activation energy observed for a given sample and magnetic field (e.g., sample D at 20.8 T or sample L at 18.4 T) is comparable to the observed variations between samples.

(2) The data for $\nu=\frac{1}{3}$ and $\frac{2}{3}$ overlap at $B\sim 15$–20 T. Furthermore, the data for $\nu=\frac{4}{3}$ and $\frac{5}{3}$ are consistent with the data for $\nu=\frac{2}{3}$ at similar magnetic fields. We therefore conclude that within experimental uncertainty, the phenomena at $\nu=\frac{1}{3}$, $\frac{2}{3}$, $\frac{4}{3}$, and $\frac{5}{3}$ result from the same energy gap above the condensed ground state. This is a plausible result from simple considerations. If higher Landau levels and the upper spin-split subband are ignored ($\Delta \ll g^*\mu_B B$ and $\hbar\omega_c$), then the $\frac{1}{3}$ and $\frac{2}{3}$ states are electron-hole symmetric and, thus, yield identical energy gaps. The $\frac{4}{3}$ and $\frac{5}{3}$ states can be understood as the $\frac{1}{3}$ and $\frac{2}{3}$ states for the upper spin-split subband. (Note that this interpretation does not extend to the $\frac{7}{3}$ and $\frac{8}{3}$ states, for which the single-electron wave functions, which form the basis for the Laughlin many-body wave function, are different.[33])

(3) The observed pair-creation energies are much smaller than theoretically predicted. As discussed previously, the calculations yield energy gaps of the form $\Delta=C_0 e^2/\epsilon l_0$. In our experimental units, this corresponds to $\Delta=50.95 C_0 B^{1/2}$, where Δ is in kelvin and B is in telsa. For comparison, Fig. 6 contains a dashed line for $C_0=0.03$ which lies above the experimental data and yet is over a factor of 3 smaller than the theoretical Δ_{QP} result ($C_0\sim 0.10$) for an ideal 2D system.

Despite the electrical neutrality of the magneto-rotons, a calculation of the conductivity in the FQHE regime suggests that thermally activated magneto-roton can provide a channel for dissipation.[34] This yields an activation energy ${}^3\Delta/2$ equal to the magneto-roton gap Δ_{MR}. The calculated gap ($C_0\sim 0.08$) corresponds to values for ${}^3\Delta$ which are over a factor of 5 larger than the dashed line in Fig. 6. (Note that the activation energy ${}^3\Delta/2$ should be compared to *half* of the pair-creation gap Δ_{QP} but should be compared *directly* to the magneto-roton gap Δ_{MR}.[34])

(4) ${}^3\Delta$ does not follow the predicted $B^{1/2}$ magnetic field dependence. Rather, the experimental data show a finite threshold at $B\sim 5.5$ T. For higher magnetic fields, there is a smooth dependence on magnetic field which can be described as a roughly linear increase in ${}^3\Delta$ up to $B\sim 18$ T, followed by a weaker magnetic field dependence towards $B=30$ T.

B. Behavior of ${}^3\Delta$ with decreasing mobility

Negative gate biases were applied to two samples (D and M) with $\mu_0=300\,000$ cm^2/V s, to achieve reduced mobilities calculated to be 100 000 to 250 000 cm^2/V s using the relation $\mu\propto n^{\chi}$. The five resulting pair-creation energies, plotted in Fig. 7, are consistent with a reduction of the energy gap and an increase in the threshold magnetic field with decreasing electron mobility. These results demonstrate that the data in Fig. 6 can only be regarded as universal within a class of samples of similar mobility and growth parameters. Samples which

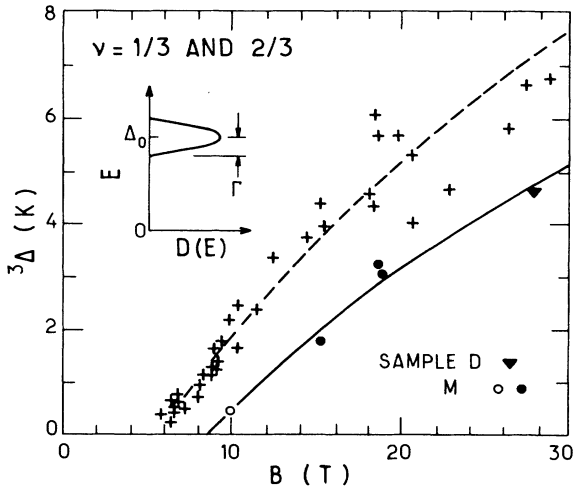

FIG. 7. The pair-creation energy of the thirds for intermediate mobilities, achieved by negatively biasing two high-mobility samples. The open and solid symbols correspond to $\nu=\frac{2}{3}$ and $\frac{1}{3}$, respectively. The data from Fig. 4 are included as "+". The solid and dashed lines correspond to fits to the phenomenological model for the effects of disorder, as illustrated in the inset and described in the text.

differ considerably from these parameters show a different behavior as substantiated by the wide range of activation energies reported in the literature.[4,5,8,9] However, the data points of Fig. 7 are consistent with a formula based on a simple phenomenological model[2] depicted in the inset to Fig. 7. In the presence of disorder, the excitation energy level is broadened. Transport then sets in below Δ_0 at pair production energy,

$$ {}^3\Delta(\mu,B)\cong\Delta_0(\mu,B)-\Gamma(\mu)=C_0(\mu)(e^2/\epsilon l_0)-\Gamma(\mu)\ , $$

where $\Gamma(\mu)$ is the half width of the distribution assumed to be magnetic field independent.

The five data of intermediate mobilities (100 000–250 000 cm^2/V s) are consistent with $C_0(100$–$250)=0.040$ and $\Gamma(100$–$250)=5.9$ K (solid line in Fig. 7). The high-mobility data from Fig. 6 are included as crosses in Fig. 7. A relatively satisfactory least-squares fit to this high-mobility data yields $C_0(400$–$1000)=0.049$ and $\Gamma(400$–$1000)=6.0$ K (dashed line in Fig. 7). Despite the quality of the fits, it should be noted that this simple model should not work when $\Gamma(\mu)\gtrsim {}^3\Delta(\mu,B)$, for which thermal excitations do not yield a simple exponential behavior.

To date, there have been two independent attempts to fit the experimental activation energy results by modeling the disorder potential.[35,36] Of greatest importance with regard to the experiments, these calculations establish the existence of a finite threshold magnetic field in the presence of disorder. Unfortunately, both calculations require adjustable parameters to achieve agreement with the experimental data of Fig. 6. Their fitted curves, which resemble the dashed curve in Fig. 7 from our phenomenological model, may well represent a practical limit for agreement between theoretical calculations and

activation energy experiments, given the ignorance of the disorder potential in any given sample.

C. Low-mobility results

We extend the range of mobility by studying three samples (*H*, *I*, and *J*) of low mobility $\mu_0 < 150\,000$ cm^2/V s). Figure 8 contains the data from the $\frac{1}{3}$ and $\frac{2}{3}$ minima of one of these samples. These results are more ambiguous than the results from the high-mobility samples. Meaningful fits using the sum of two conduction mechanisms, as discussed previously, are not possible here, due to the reduced dynamic range of the data. However, it is illuminating to attempt to fit the low-mobility data with individual conduction formulas. From observations on the high-mobility samples, we expect that the effects due to hopping conduction will be largest at high magnetic fields. Indeed, eight out of nine of the sets of data for $B > 23$ T are consistent with the Ono hopping formula alone over the entire temperature range. (The sole exception is an unusual and probably incorrect data set which fits none of the three formulas.) To demonstrate the quality of the fit to the Ono formula, we show Fig. 9 which contains the data on $\nu = \frac{1}{3}$ at $B = 25.2$ T. This is the set with the greatest dynamic range, chosen to best distinguish among the three low-T formulas. While the data in Fig. 9 seem sufficient to distinguish among them, it is possible that the magnetic field noise causes local heating in either the 2D layer or the carbon resistor thermometer, introducing errors in our thermometry at the lowest temperatures. However, even if all points below 125 mK are rejected as unreliable, the remaining part of the curve still points towards the Ono formula as providing the best fit. We find, therefore, that at high magnetic fields the observed conduction is consistent with the functional form of the Ono hopping formula.

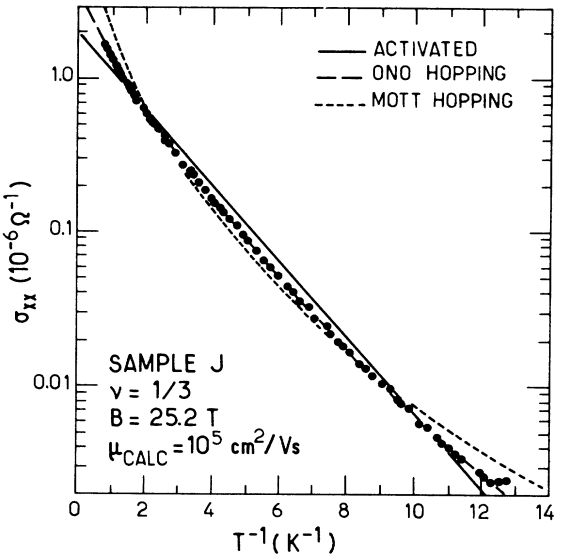

FIG. 9. Temperature dependence of the σ_{xx} minima for a low-mobility sample. The three lines show least-squares fits to the three conduction formulas.

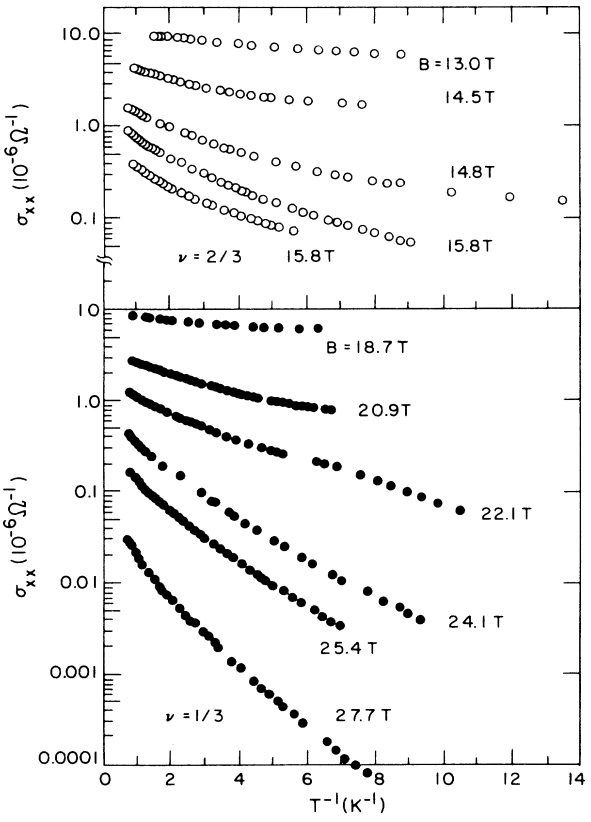

FIG. 8. Overview of temperature dependence of the σ_{xx} minima for a low-mobility sample (sample I) for magnetic fields from 13.0 to 27.7 T. The data represented by open and solid circles is from $\nu = \frac{2}{3}$ and $\frac{1}{3}$, respectively.

At lower magnetic fields, we expect that the observed conduction will include components from both hopping and activated conduction. This "crossover regime" has a somewhat increased curvature, as observed on the high-mobility samples. At the lowest magnetic fields, we may reach a regime in which only the activated conduction is observed. This proposed sequence is consistent with what is observed at lower magnetic fields on the three low-mobility samples.

The implications of this interpretation are several. Firstly, the functional form of the Ono formula, which was derived for 2D hopping in the presence of a magnetic field, is substantiated by our experiments. Also, we now have experimental support for our attribution of the low-T deviations observed in the high-mobility samples to quasiparticle localization as described by the Ono formula.

The fitted values of $T_{\rm Ono}$ from the three low-mobility samples are plotted versus magnetic field in Fig. 10.[37] If we assume that the quasiparticle density of states at a given fractional filling is independent of magnetic field, $T_{\rm Ono}$ should be linear in magnetic field. While the data of Fig. 10 cannot suggest a linear dependence, we fit a straight line to it for an order-of-magnitude determination of the density of quasiparticle states. From the

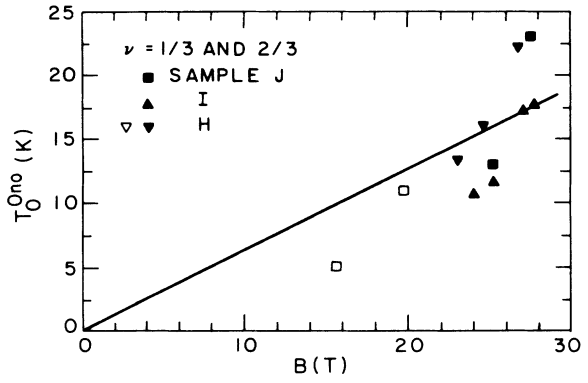

FIG. 10. T_{Ono} vs magnetic field for the low-mobility samples. The open and solid symbols correspond to $\nu=\frac{2}{3}$ and $\frac{1}{3}$, respectively. The solid line corresponds to $D(E_F)\sim 3\times 10^{12}$ meV^{-1}cm^{-2}. By contrast, the electron density of states in zero magnetic field is 2.9×10^{10} meV^{-1}cm^{-2} for GaAs.

slope of this line, the density of states at the Fermi energy is $D_{1/3,2/3}(E_F)\sim 3\times 10^{12}$ meV^{-1}cm^{-2} for $\nu=\frac{1}{3}$ and $\frac{2}{3}$. This is 2 orders of magnitude larger than the electron density of states in zero magnetic field, which should serve as an approximate upper limit independent of whether our experiment is probing electrons or quasiparticles. Similar, although smaller, discrepancies have been noted for electrons in the IQHE regime on GaAs/$Al_xGa_{1-x}As$ heterojunctions[27] and InP/$In_xGa_{1-x}As$ heterojunctions.[28]

D. Absence of narrow-channel effects

The high-mobility sample *G*, is a narrow-channel Hall bridge of dimensions 11 μm $\times$450 μm, on which we investigate the possible channel width dependence of the pair-creation energy. An unusual size effect has been reported in the IQHE regime, characterized by saw-toothed quantum oscillations in ρ_{xx} and asymmetric plateaus in ρ_{xy}.[38]

Our narrow-channel sample does exhibit this saw-tooth size effect in both the IQHE and FQHE regimes. However, no resultant variation on the pair-creation energy at $\nu=\frac{1}{3}$ and $\frac{2}{3}$ is observed: the pair-creation data, contained in Table II, are consistent with the data in Fig. 6 on samples of similar mobility.

TABLE II. Pair-creation energy from the narrow-channel Hall sample (sample *G*; channel dimensions of 11 μm $\times$ 450 μm). These results are consistent with the data of Fig. 6 from wide-channel samples of similar mobility.

ν	B (T)	$^3\Delta$ (K)
$\frac{2}{3}$	9.2	1.1
$\frac{2}{3}$	10.7	1.7
$\frac{1}{3}$	20.3	6.9
$\frac{1}{3}$	21.5	6.5

E. Filling factors $\frac{2}{5}$ and $\frac{3}{5}$

We turn our attention now to filling factors other than the thirds. For our high-mobility samples, the only other ρ_{xx} minima which are sufficiently well developed for a meaningful study are minima at $\nu=\frac{2}{5}$ and $\frac{3}{5}$ at higher magnetic fields. The data in Fig. 11 reveal a much smaller temperature dependence at $\nu=\frac{2}{5}$ and $\frac{3}{5}$ than observed on the thirds. Within our temperature range, ρ_{xx} and σ_{xx} change by less than 2 orders of magnitude. Furthermore, the interpretation of the observed temperature dependence as indicating activated conduction is ambiguous. Nevertheless, we approach this data with the same models used with the thirds. The data on the fifths can be fitted with activated conduction at high temperature and any of the three discussed models at low temperature (solid line in Fig. 12). The model chosen to fit the low-T data has a moderate influence (15% typically) on the resulting high-T pair-creation energy. As with the thirds, attempts to fit the data over the entire temperature range with a single conduction formula are unsuccessful. The dashed lines in Fig. 12 give each component for a combination of activated conduction and Ono hopping model. Note that the activation energy from the model differs dramatically from a straight-line fit to the high-T data.

The entire body of data for the fifths indicates a magnetic field evolution similar to that of the thirds. The 20 sets of experimental data (Fig. 13) suggest a single pair-creation energy $^5\Delta$, for $\nu=\frac{2}{5}$ and $\frac{3}{5}$, which increases monotonically with magnetic field. If the pair-creation energies at $\nu=p/q$ scale as $q^{-5/2}$, the ratio $^5\Delta/^3\Delta=0.28$ and $C_0\sim 0.03$ for Δ_{QP}. Experimentally, $^5\Delta/^3\Delta\sim 0.4$ and Fig. 13 contains a dashed line for $C=0.015$, a factor of 2 below the theoretical result for the ideal 2D system.

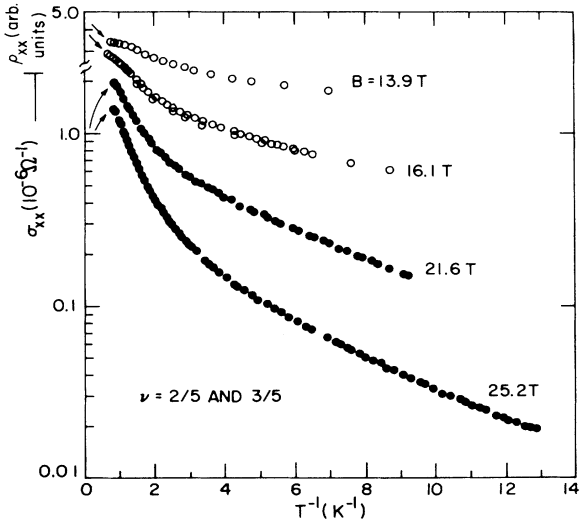

FIG. 11. Overview of temperature dependence of the ρ_{xx} and σ_{xx} minima for the fifths with magnetic fields from 13.9 to 25.2 T. The open and solid symbols are from $\nu=\frac{3}{5}$ and $\frac{2}{5}$, respectively.

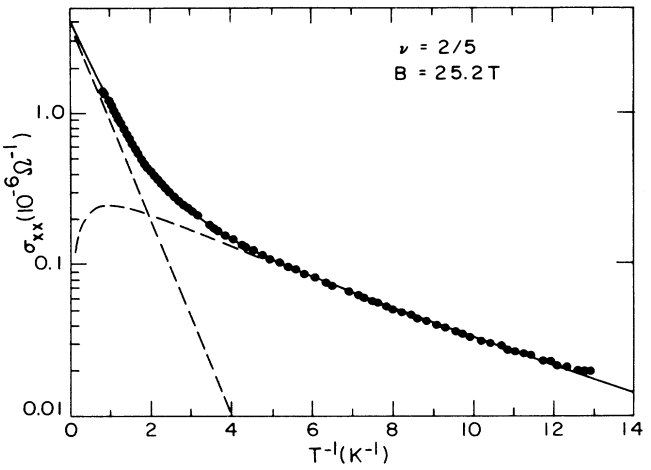

FIG. 12. Temperature dependence of the minimum at $\nu=\frac{2}{5}$ at $B=25.2$ T. The dashed lines indicate the two components of the activated conduction-Ono hopping conduction model; the solid line is their sum. Note that the activation energy (high-T, dashed line) does not correspond to a line through the high-T data, in contrast with the data on the thirds minima.

From Fig. 11 it is clear that the onset of the low-T deviation occurs at higher temperature for the fifths than for the thirds, despite the smaller activation energies. The fifths seem to be more affected by the potential fluctuations, resulting in a more significant low-T deviation due to localization. The plot of $T_{\rm Ono}$ versus B for the fifths (Fig. 14) shows the resulting smaller magnitude of $T_{\rm Ono}$ for the fifths than for the thirds. The solid line in Fig. 14 corresponds to $D_{2/5,3/5}(E_F)\sim 1.9\times 10^{13}$ meV^{-1}cm^{-2}. This density of states is a factor of 7 larger than derived for the thirds and, as in this former case, is unphysically large.

V. DISCUSSION

The activation energy results of the high-mobility samples demonstrate that there exists a substantial

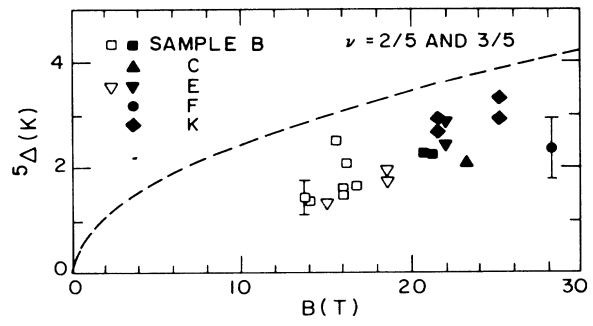

FIG. 13. The pair-creation energy for the fifths vs magnetic field for high-mobility samples. The open and solid symbols correspond to $\nu=\frac{3}{5}$ and $\frac{2}{5}$, respectively. The dashed line corresponds to ${}^5\Delta=0.015e^2/\epsilon l_0$, a factor of 2 smaller than the calculated pair-creation energy gap for an ideal two-dimensional system.

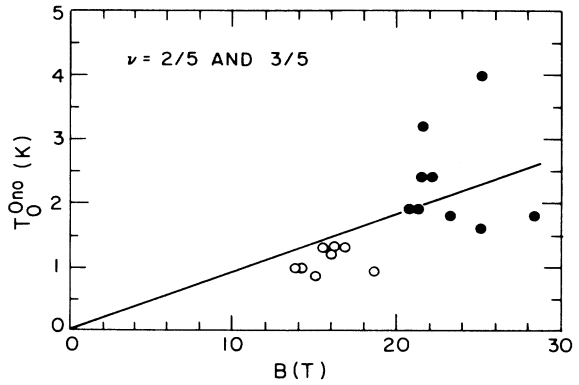

FIG. 14. $T_{\rm Ono}$ vs magnetic field for the fifths from high-mobility samples. The open and solid symbols correspond to the $\nu=\frac{3}{5}$ and $\frac{2}{5}$ minima, respectively. The solid line corresponds to $D(E_F)\sim 2\times 10^{13}$ meV^{-1}cm^{-2}.

discrepancy between experiment and theory which remains to be explained. The admixture of higher Landau levels destroys electron-hole symmetry and reduces the energy gaps in the FQHE. Yoshioka[31] finds the reduction for a four-electron system to be $\sim 15\%$ at $B=5.5$ T. This reduction decreases as magnetic field increases or if finite thickness of the 2D system is included in the calculation. Thus, Landau-level mixing cannot explain our discrepancies. The finite thickness of the electronic system weakens the short-range Coulomb interaction between electrons. The resulting reduction in the energy gaps increases with magnetic field, which could qualitatively account for the observed weaker magnetic field dependence of ${}^3\Delta$ for $B\gtrsim 18$ T. However, Zhang and Das Sarma[39] calculate a reduced gap that remains about a factor of 3 above our experimental results. Yoshioka[31] considers finite layer thickness and admixture of higher Landau levels together and finds a reduced gap about a factor of 2 larger than experiment. He also finds the energy gaps at $\nu=\frac{1}{3}$ and $\frac{2}{3}$ to be different in the absence of electron-hole symmetry. For $15\lesssim B\lesssim 20$ T, where our $\frac{1}{3}$ and $\frac{2}{3}$ data overlap, ${}^3\Delta$ should be ~ 1 K larger for $\nu=\frac{2}{3}$ than for $\nu=\frac{1}{3}$. The data of Fig. 6 show no evidence of this; however, the expected difference is of the same magnitude as the experimental uncertainties.

It has been suggested that the elementary excitations above the Laughlin ground state at lower magnetic fields may consist of spin-reversed quasiparticles.[40,41] From calculations on four- and five-electron systems, the spin-reversed quasielectron and spin-polarized quasihole production is found to be energetically favorable for magnetic fields less than ~ 12 T. In this range of magnetic field, the Zeeman energy is dominant and, thus, the energy gap scales linearly with magnetic field. Finite layer thickness is included and the calculation finds a slope for the linear dependence which is in very close agreement with the roughly linear dependence of ${}^3\Delta$ observed for $5.5\lesssim B\lesssim 18$ T. However, the calculated energy gap exhibits no finite magnetic field threshold and remains about 50% higher than the experimental values at high

magnetic fields, where the agreement is best.

Although each model reduces the discrepancy with the observed magnitudes of the energy gaps, neither admixture of higher Landau levels, nor finite layer thickness, nor spin-reversed quasiparticles can account for the observed finite magnetic field threshold. The presence of disorder and subsequent thermal excitation to a broadened energy level provides a qualitative explanation for the reduced magnitudes as well as for the finite threshold field.[2] Experimentally, effects of disorder can be probed by studying samples of widely different mobilities. Unfortunately, the mobility range of available samples which exhibit the FQHE is severely limited. Also, the mobility of a given sample provides only limited information about the disorder potential, which is the physically relevant quantity. Different scattering mechanisms could limit mobility in samples with widely varying parameters, such as background impurity concentration and spacer-layer thickness, yielding no clear mobility dependence of the activation energy. Recent theoretical work[35,36] assesses the effects of disorder on the energy gaps in the FQHE reaching rather satisfactory agreement with our experimental results, including the existence of a finite-field threshold for the development of the energy gap.

VI. CONCLUSIONS

We have presented the results from our study of magnetotransport in the FQHE regime on samples of varying mobility. In our samples of highest mobility, we find a single pair creation energy ${}^3\Delta$ for $\nu=\frac{1}{3}$, $\frac{2}{3}$, $\frac{4}{3}$, and $\frac{5}{3}$ in magnetic fields up to 28 T which has a smaller magnitude and different magnetic field dependence than expected from calculations of the ideal 2D system. Most prominent is the existence of a finite magnetic field threshold. As mobility is decreased, the magnitude of ${}^3\Delta$ decreases and the magnetic field threshold increases. Deviations from activated conduction at the lowest temperatures are attributed to hopping conduction in a magnetic field. Data from low-mobility samples are consistent with this interpretation. They are well described over the entire experimental temperature range by a functional dependence derived by Ono, although a large quantitative discrepancy remains. We have also found a single pair-creation energy ${}^5\Delta$ for $\nu=\frac{2}{5}$ and $\frac{3}{5}$ on our high-mobility samples. The ratio ${}^5\Delta/{}^3\Delta$ is at variance with simple theoretical considerations.

ACKNOWLEDGMENTS

We thank P. A. Wolff and L. Rubin at the Francis Bitter National Magnet Laboratory for assistance and support. We would also like to thank K. Baldwin for technical support. The Francis Bitter National Magnet Laboratory is supported by the National Science Foundation through its Division of Materials Research. One of us (G.S.B.) is grateful to the Fannie and John Hertz Foundation for financial support. Another one of us (D.C.T.) is supported by the National Science Foundation through Grant No. DMR-82-12167.

*Present address: AT&T Bell Laboratories, Murray Hill, New Jersey 07974.

†Also at the Francis Bitter National Magnet Laboratory, Cambridge, MA 02139.

‡Present address: Gain Electronics Corp., Somerville, NJ 08876.

[1]D. C. Tsui, H. L. Stormer, and A. C. Gossard, Phys. Rev. Lett. **48**, 1559 (1982).

[2]A. M. Chang, M. A. Paalanen, D. C. Tsui, H. L. Stormer, and J. C. M. Hwang, Phys. Rev. B **28**, 6133 (1983), and unpublished data.

[3]D. C. Tsui, H. L. Stormer, J. C. M. Hwang, J. S. Brooks, and M. J. Naughton, Phys. Rev. B **28**, 2274 (1983).

[4]G. Ebert, K. von Klitzing, J. C. Maan, G. Remenyi, C. Probst, G. Weimann, and W. Schlapp, J. Phys. C **17**, L775 (1984).

[5]S. Kawaji, J. Wakabayashi, J. Yoshino, and H. Sakaki, J. Phys. Soc. Jpn. **53**, 1915 (1984).

[6]G. S. Boebinger, A. M. Chang, H. L. Stormer, and D. C. Tsui, Phys. Rev. Lett. **55**, 1606 (1985).

[7]G. S. Boebinger, A. M. Chang, H. L. Stormer, D. C. Tsui, J. C. M. Hwang, A. Cho, C. Tu, and G. Weimann, Surf. Sci. **170**, 129 (1986).

[8]J. Wakabayashi, S. Kawaji, J. Yoshino, and H. Sakaki, Surf. Sci. **170**, 136 (1986).

[9]R. G. Clark, R. J. Nicholas, A. Usher, C. T. Foxon, and J. J. Harris, Surf. Sci. **170**, 141 (1986).

[10]I. V. Kukushkin and V. B. Timofeev, Surf. Sci. **170**, 148 (1986).

[11]J. Wakabayashi, S. Kawaji, J. Yoshino, and H. Sakaki, J. Phys. Soc. Jpn. **55**, 1319 (1986).

[12]I. V. Kukushkin and V. B. Timofeev, Pis'ma Zh. Eksp. Teor. Fiz. **44**, 179 (1986) [JETP Lett. **44**, 228 (1986)].

[13]R. B. Laughlin, Phys. Rev. Lett. **50**, 1395 (1983).

[14]F. D. M. Haldane, Phys. Rev. Lett. **51**, 605 (1983).

[15]R. B. Laughlin, Surf. Sci. **142**, 163 (1984).

[16]B. I. Halperin, Phys. Rev. Lett. **52**, 1583 (1984).

[17]S. M. Girvin, A. H. MacDonald, and P. M. Platzman, Phys. Rev. Lett. **54**, 581 (1985); Phys. Rev. B **33**, 2481 (1986).

[18]F. D. M. Haldane and E. H. Rezayi, Phys. Rev. Lett. **54**, 237 (1985).

[19]G. Fano, F. Ortolani, and E. Colombo, Phys. Rev. B **34**, 2670 (1986).

[20]R. Morf and B. I. Halperin, Phys. Rev. B **33**, 2221 (1986).

[21]W. P. Su, Phys. Rev. B **32**, 2617 (1985).

[22]H. L. Stormer, Surf. Sci. **132**, 519 (1983).

[23]J. C. M. Hwang, A. Kastalsky, H. L. Stormer, and V. G. Keramidas, Appl. Phys. Lett. **44**, 802 (1984).

[24]H. L. Stormer, A. C. Gossard, and W. Wiegmann, Appl. Phys. Lett. **39**, 493 (1981).

[25]G. S. Boebinger, Ph.D. thesis, Massachusetts Institute of Technology, 1986; in *The Physics of the Two Dimensional Electron Gas*, Proceedings of NATO Advanced Study Institute, Antwerp, Belgium, 1986 (unpublished).

[26]M. J. Naughton, S. Dickenson, R. C. Samaratunga, J. S. Brooks, and K. P. Martin, Rev. Sci. Instrum. **54**, 1529 (1983).
[27]G. Ebert, K. von Klitzing, C. Probst, E. Schuberth, K. Ploog, and G. Weimann, Solid State Commun. **45**, 625 (1983).
[28]Y. Guldner, J. P. Hirtz, A. Briggs, J. P. Vieren, M. Voos, and M. Rezeghi, Surf. Sci. **142**, 179 (1984).
[29]Y. Ono, J. Phys. Soc. Jpn. **51**, 237 (1982).
[30]N. F. Mott and E. A. Davis, *Electronic Properties in Non-Crystalline Materials,* 2nd ed. (Clarendon, Oxford, 1979).
[31]D. Yoshioka, J. Phys. Soc. Jpn. **55**, 885 (1986).
[32]J. Ihm and J. C. Phillips, J. Phys. Soc. Jpn. **54**, 1506 (1985).
[33]A. H. MacDonald, Phys. Rev. B **30**, 3550 (1984).
[34]P. M. Platzman, S. M. Girvin, and A. H. MacDonald, Phys. Rev. B **32**, 8458 (1985).
[35]A. H. MacDonald, K. L. Liu, S. M. Girvin, and P. M. Platzman, Phys. Rev. B **33**, 4014 (1985).
[36]A. Gold, Europhys. Lett. **1**, 241 (1986); **1**, 479(E) (1986); and unpublished.
[37]The magnitudes of T_{Ono} from the high-mobility samples are consistent with this data. However, they exhibit much greater random scatter (up to a factor of 6 at a given magnetic field), resulting from the lower accuracy of determining a fit solely from the low-T deviation.
[38]H. Z. Zhang, K. K. Choi, D. C. Tsui, and G. Weimann, Phys. Rev. Lett. **55**, 1144 (1985).
[39]F. C. Zhang and S. Das Sarma, Phys. Rev. B **33**, 2903 (1986).
[40]T. Chakraborty, P. Pietilainen, and F. C. Zhang, Phys. Rev. Lett. **57**, 130 (1986).
[41]T. Chakraborty, Phys. Rev. B **34**, 2926 (1986).